2022 IEEE International Conference on Bioinformatics and Biomedicine (BIBM) | 978-1-6654-6819-0/22/$31.00 ©2022 IEEE | DOI: 10.1109/BIBM55620.2022.9994951

ImageALCAPA: A 3D Computed Tomography Image Dataset for Automatic Segmentation of Anomalous Left Coronary Artery from Pulmonary Artery

An Zeng*, Chenxi Mi*, Dan Pan†, Qing Lu‡, Xiaowei Xu§
*School of Computer Science, Guangdong University of Technology, Guangzhou, China.
†Department of Computer Science, Guangdong Polytechnic Normal University, Guangzhou, China
Email: pandan@gpnu.edu.cn (corresponding author)
‡Department of Computer Science and Engineering, University of Notre Dame, IN, US
§Guangdong Provincial People's Hospital, Guangdong Academy of Medical Sciences, Guangzhou, China
Email: xiao.wei.xu@foxmail.com (corresponding author)

***Abstract*—Anomalous left coronary artery from pulmonary artery (ALCAPA) is a serious cardiac anomaly, and surgical repair is the main treatment for ALCAPA patients in clinical practice. Recently, 3D printing has been widely adopted in the surgical planning of ALCAPA, which can give surgeons an intuitive structure of the heart especially the coronary arteries. However, before 3D printing is conducted, experienced radiologists need to manually segment the coronary arteries on computed tomography angiography (CTA) images, which is time-consuming, tedious and biased. On the other hand, automatic coronary artery segmentation with normal structures has been extensively studied in the community, but cannot be effectively applied to ALCAPA due to the significant variation of coronary artery structure in ALCAPA. In this paper, we propose ImageALCAPA, the first 3D CTA image dataset of ALCAPA. The proposed dataset contains 30 ALCAPA CTA images, which is of decent size compared with existing medical imaging datasets. We further propose a baseline method that performs multi-task 2D-3D ensemble for automatic segmentation of ALCAPA. It is shown by experiment that our baseline method outperforms popular existing works on coronary artery segmentation. However, as the highest average Dice Similarity Coefficient o f c oronary arteries is merely 65%, there is still much room for improvement. To facilitate further research on this challenging problem, our dataset and codes are released to the public [1].**

***Index Terms*—Anomalous left coronary artery from pulmonary artery, Medical image segmentation, Computed tomography, Dataset**

I. Introduction

Anomalous left coronary artery from pulmonary artery (ALCAPA) is a serious congenital cardiac malformation, [2] which can induce heart failure in the early period and finally results in death. It is present in 0.5% of children with congenital heart disease [3].

The main treatment of ALCAPA is surgical repair [4], which is rather challenging as surgeons needs to restore the anomalous coronary artery to the right position with a correct connection to other anatomies [5]. In recent years, 3D printing has been widely adopted in surgical planning of ALCAPA [6], [7] to assist surgeons. However, before 3D printing is conducted, experienced radiologists need to perform manual segmentation of the heart anatomies especially the coronary arteries, which is time-consuming, tedious and introduces bias by clinical experts. Therefore, the manual segmentation requires a significant amount of resources and time [7], and automatic segmentation of coronary arteries in ALCAPA computed tomography angiography (CTA) images is needed.

During the past decade, various deep learning methods have been proposed to automatically extract coronary arteries with normal structures from CTA. In 2016, Moeskops et al. [8] demonstrated that a single CNN architecture can be used for coronary vessel segmentation. Kjerland et al. [9] applied two neural networks trained on aorta segmentation and coronary segmentation respectively to segment the complete coronary tree. Wolterink et al. [10] adopted graph neural networks (GCNs) to predict the spatial location of vertices in a tubular surface mesh that segments the coronary artery lumen. Recently, Kong et al. [11] proposed a tree-structured convolutional gated recurrent unit (ConvGRU) model to learn the anatomical structure of the coronary artery.

However, compared with coronary arteries with normal structures, coronary arteries in ALCAPA have three characteristics. First, ALCPA usually presents in infants with small vessel size and increased heart rates. Second, we notice that normal coronary arteries have relatively common anatomical structures, while in ALCAPA their structures vary significantly from patient to patient. Third, the right coronary artery (RCA) is obviously larger than the left coronary artery (LCA) in ALCAPA, which leads to data imbalance and makes the segmenting LCA difficult. Although a great deal of effort has been made to the automatic segmentation of coronary arteries in CTA, study in the segmentation of coronary artery ALCAPA still remains absent from the literature.

In this paper, we present ImageALCAPA, the first 3D CTA

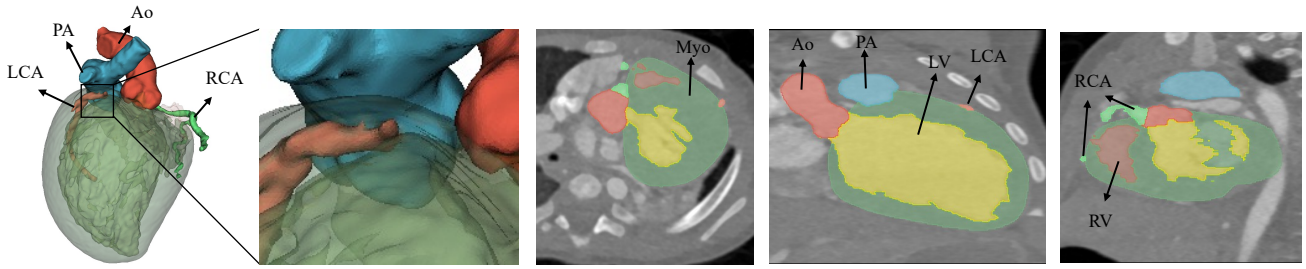

Fig. 1. Visualization of segmentation labels in imageALCAPA.

TABLE I
CHARACTERISTICS OF THE IMAGEALCAPA DATASET

Parameters	N
Sex = Female (%)	18 (60%)
Age ($Mean \pm SD$)	7.19 ± 13.06
Spacing between slice (mm)	0.75
Size of the images ($pixels$)	$512 \times 512 \times (206 - 518)$
Typical voxel size (mm^3)	$0.25 \times 0.25 \times 0.5$

image dataset of ALCAPA. In this dataset, multiple anatomical structures have been annotated including myocardium (Myo), left ventricle (LV), right ventricle (RV), pulmonary artery (PA) and aorta (Ao), LCA, and RCA. ImageALCAPA contains 30 ALCAPA CTA images. We also propose a baseline method that performs multi-task 2D-3D ensemble for automatic segmentation of ALCAPA. Experimental results show that the baseline method outperforms popular existing works on coronary artery segmentation using imageALCAPA. However, as the highest average Dice Similarity Coefficient of coronary arteries is merely 65%, there is still much room for improvement. To facilitate further research on this challenging topic, our dataset and codes are released to the public [1].

II. THE IMAGEALCAPA DATASET

The ImageALCAPA dataset totally consists of 30 3D CTA images gathered from Guangdong Provincial Peoples' Hospital from June 17, 2016, to August 8, 2021. These images are acquired by a SOMATOM Definition Flash CT machine. The details of the ImageALCAPA dataset is listed in Table I. All the images are pre-operative ALCAPA CTA images whose top and bottom are around the neck and the brachiocephalic vessels, respectively, in the axial view. The segmentation labeling is performed by a team of two cardiovascular radiologists who have extensive experience in ALCAPA. For each image, one radiologist fulfills the labelling while the other verifies it afterwards. The segmentation includes seven substructures: Myo, LV, RV, PA, Ao, LCA, and RCA, and the labelling of each image goes by 1-1.5 hours. An example of the segmentation labels including the 3D model and labels in three sections is shown in Fig. 1, where the left coronary artery arises abnormally from the pulmonary artery.

III. METHOD

A. Overview

The workflow of the baseline method is shown in Fig. 2, which includes three modules: 2D segmentation of coronary artery, 3D segmentation of LCA and RCA, and task ensemble. The main reason of two segmentation tasks is that 3D segmentation can extract 3D context information well only with limited resolution, while 2D segmentation can only make use of the information in the current 2D slice but with the full resolution. In this way, the ensemble of the two can extract the segmentation well.

B. 2D Segmentation of Coronary Artery

We adopt 2D U-net [12] to segment coronary artery slice by slice. This network cannot exploit the 3D context information but a high resolution of each 2D slice (input size 512×512). Note because only 2D context information is considered, 2D U-net cannot recognize LCA and RCA well. As a result, the final output only includes two classes: the coronary artery and the rest. After all slices are processed, all the 2D segmentation results are reconstructed as a 3D segmented image.

C. 3D Segmentation of LCA and RCA

The 3D segmentation of LCA and RCA contains two steps: RoI extraction and RoI segmentation. Both steps are fulfilled by a modified 3D U-net [13]. The former aims to locate the target area so that the latter can focus on a smaller region, which can avoid the processing of irrelevant pixels and hence reduce the data variety. Particularly, we discussed two approaches: Approach A which considers three classes (LCA, RCA and the rest), and Approach B which considers all the eight classes. As the GPU memory is limited, the input is resized to 128×128×64. With the rough segmentation, we can obtain a bounding box containing the target classes which can be used to extract the RoI from the original input. Then the RoI is resized to 256×256×128 and fed to a 3D U-net.

D. Task Ensemble

We adopt maxi-voting for task ensemble. The final class of each pixel in an input image are dependent on the maximum value of the two models. For 2D U-Net, each image is handled separately, and only 2D context information is used. In this way, the training data size can be more than 6,000, which

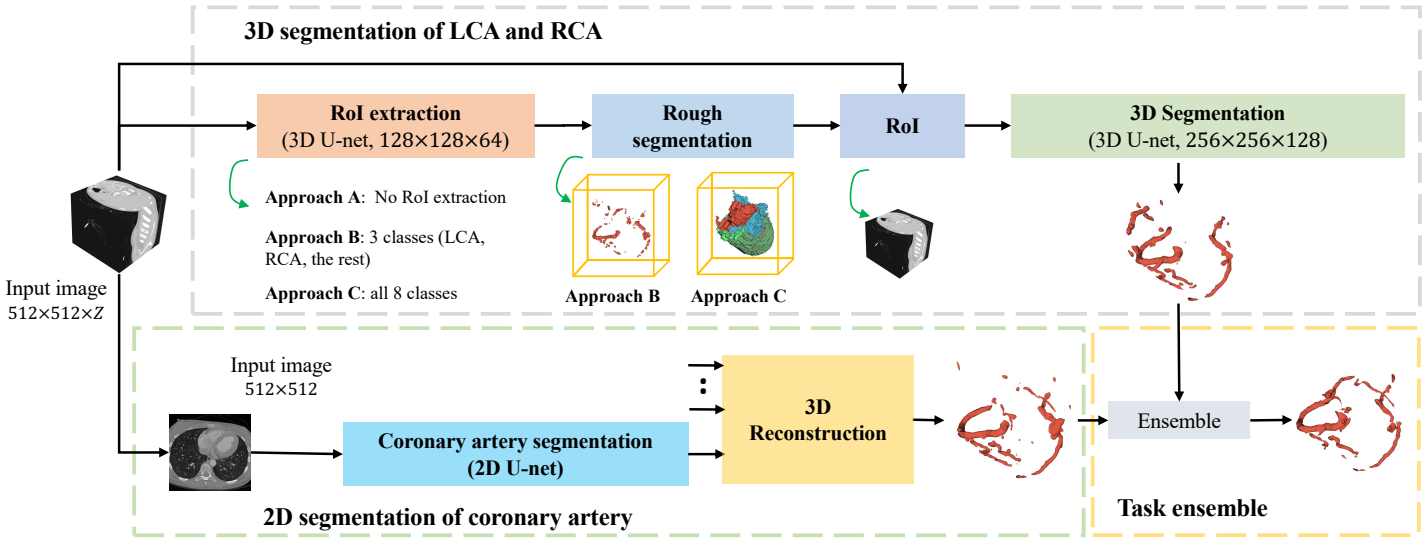

Fig. 2. Pipeline of the proposed baseline method, which performs multi-task 2D-3D ensemble. Best viewed in color.

is enough for the network training. For 3D U-Net, the dataset size is much smaller, and 3D context information is considered [14]. In this way, we combine the above two methods to make a prediction. For the post-processing, we take the largest connected component (LCC) to exclude the fragmented non-coronary artery artifacts and keep the left and right coronary arteries.

IV. Experiment and Results

In the experiment, we first perform the comparison of the baseline method and existing methods [15], [16], followed by discussing impact of other labels on coronary segmentation in Approach B.

A. Experiment Setup

All the experiments run on a Nvidia GeForce RTX 3090 GPU with 24 GB memory. Using Pytorch as the underlying framework, our implementation of the 2D U-net is based on [12], and that of the 3D modified U-net is based on [13]. For the binary segmentation task, we use the Dice loss. And for the multi-class segmentation task, we use the cross-entropy loss. The number of training epochs is 80 and 100 for 2D U-net and 3D U-net, respectively. Data normalization and augmentation is the same as [17]. The learning rate is 0.0001 and 0.001 for 2D U-net and 3D U-net, respectively. For all the methods, five-fold cross validation is performed (6 images for testing and 24 images for training). The Dice score, Sensitivity and Hausdorff distance are used for evaluation.

B. Results

1) Comparison with existing networks: Table II shows the mean and standard deviation of the three metrics of the baseline method for coronary artery segmentation. It is observed that ours using 2D U-net and Approach C achieves the optimal performance in both DSC and sensitivity. We can also see that 2D U-net obtains the best HD which is much lower than others. This maybe due to the fact that 2D U-net works on the original resolution and can usually preserve the boundaries well. Besides, it is found that Approach A (no RoI extraction, and 3D U-net is used) performs worse than the 2D U-net as it re-samples the input data to a lower resolution, and Approach B performs worst on the coronary segmentation. A possible reason is that in RoI segmentation, the input has been resized to avoid excessive memory consumption and over-fitting, which makes the coronary artery thinner or even partially missing. As a result, the predicted RoI is unable to include the whole coronary arteries. Approach C obtains a much higher DSC as it used all labels to get a more accurate RoI and avoid the above problem.

TABLE II
Comparison of the performances on the testing data between our proposed method and other methods.

Methods	DSC (%)	Sens (%)	HD (mm)
2D U-net	0.58±0.13	0.52±0.17	**44.77**±20.68
Approach A (No RoI extraction)	0.51±0.13	0.48±0.16	66.78±44.89
Approach B [15] [16]	0.47±0.15	0.48±0.17	87.43±60.29
Approach C [15] [16]	0.59±0.11	0.54±0.13	55.98±35.79
Ours (2D U-net + Approach A)	0.60±0.12	0.63±0.17	56.67±36.79
Ours (2D U-net + Approach B)	0.57±0.15	0.59±0.17	84.92±76.55
Ours (2D U-net + Approach C)	**0.65**±0.11	**0.65**±0.16	53.64±34.34

A similar trend can be found in our proposed baseline method with three configurations: 2D U-net with Approach C obtains the best performance and that with Approach B gets the worst performance. We can also notice that our baseline method with three configurations obtains improved performance by taking consideration of 2D U-net, and the gaps narrows down as the performance gets higher. For example, Approach B has the lowest performance among the three

TABLE III
COMPARISONS OF DIFFERENT LABELS' IMPACT ON THE SEGMENTATION OF CORONARY ARTERIES.

Labels	DSC (%)	Sensitivity (%)	HD (mm)
None	0.65±0.11	0.65±0.16	53.64±34.34
Myo	0.53±0.12	0.53±0.14	59.79±41.55
LV	0.55±0.14	0.52±0.16	57.07±36.00
RV	0.57±0.10	0.55±0.13	61.86±37.46
Ao	0.51±0.12	0.46±0.14	61.69±34.18
PA	0.54±0.13	0.50±0.14	60.99±43.17
All	0.54±0.10	0.58±0.16	56.58±41.33

approaches. In our baseline method, the improvement of 2D U-net with Approach B over Approach B is about 0.10 in DSC, which is the highest improvement. Note that Approach B and C [15] [16] have been widely adopted in segmentation of coronary arteries with normal structures.

Note that existing methods [15] [16] on coronary artery with normal structure can achieve a high DSC of around 0.90. However, these methods can only obtain a DSC less than 0.60, which shows the segmentation of coronary artery in ALCAPA is quite different and also a rather challenging task. In addition, the results also indicate that our baseline method is a powerful baseline method.

2) Performance with added labels: We also perform experiments to study the impact of adding other labels to the segmentation performance of small coronary arteries. Table III shows the results. We can notice that the surrounding labels tend to cause an adverse effect on the segmentation of coronary arteries, which may be caused by data imbalance. Particularly, the coronary artery labels are relatively small compared with the added labels like LV and RV. The machine learning classifier tends to be more biased towards the majority classes, causing bad segmentation of the minority classes.

V. CONCLUSION

In this paper, we introduce the ImageALCAPA dataset to the community, which is the first 3D CTA image dataset of ALCAPA with annotation of myocardium (Myo), left ventricle (LV), right ventricle (RV), aorta (Ao) and pulmonary artery (PA), left coronary artery (LCA), and right coronary artery (RCA). We further propose a baseline method based on multi-task 2D-3D ensemble for automatic segmentation of ALCAPA. Experiment results show that the baseline method can achieve superior results over existing works on segmentation of coronary artery with normal structures. However, the segmentation accuracy is only 65%, which leaves large room for improvement and proves the challenge of our dataset. We hope that the open-sourced code of our baseline method and dataset can encourage the community to tackle this problem.

ACKNOWLEDGMENT

This study was supported by the Science and Technology Planning Project of Guangdong (Grant Nos.2019A050510041, 2021A1515012300 and 2021B0101220006), National Natural Science Foundation of China (Grant Nos. 61976058, 61772143), Science and Technology Planning Project of Guangzhou (Grant Nos.202103000034, 202206010007 and 202002020090) and Science and Technology Planning Project of Yunnan (Grant Nos.202102AA100012).

REFERENCES

[1] https://github.com/XiaoweiXu/ImageALCAPA-A-3D-Computed-Tomography-Image-Dataset-for-Automatic-Segmentation-of-ALCAPA.
[2] A. Murthy, G. Y. Kim, H. Khawaja, and L. Sullenberger, "Anomalous origin of the left coronary artery from pulmonary artery a late presentation—case report and review of literature," *Journal of Cardiology Cases*, vol. 9, no. 1, pp. 22–25, 2014.
[3] A. Dodge-Khatami, C. Mavroudis, and C. L. Backer, "Anomalous origin of the left coronary artery from the pulmonary artery: collective review of surgical therapy," *The Annals of thoracic surgery*, vol. 74, no. 3, pp. 946–955, 2002.
[4] E. Peña, E. T. Nguyen, N. Merchant, and C. Dennie, "Alcapa syndrome: not just a pediatric disease," *Radiographics*, vol. 29, no. 2, pp. 553–565, 2009.
[5] H. WESSELHOEFT, J. Fawcett, and A. L. JOHNSON, "Anomalous origin of the left coronary artery from the pulmonary trunk: its clinical spectrum, pathology, and pathophysiology, based on a review of 140 cases with seven further cases," *Circulation*, vol. 38, no. 2, pp. 403–425, 1968.
[6] R. Javan, D. Herrin, and A. Tangestanipoor, "Understanding spatially complex segmental and branch anatomy using 3d printing: liver, lung, prostate, coronary arteries, and circle of willis," *Academic radiology*, vol. 23, no. 9, pp. 1183–1189, 2016.
[7] M. Lee, S. Moharem-Elgamal, R. Beckingham, M. Hamilton, N. Manghat, E. G. Milano, C. Bucciarelli-Ducci, M. Caputo, and G. Biglino, "Evaluating 3d-printed models of coronary anomalies: a survey among clinicians and researchers at a university hospital in the uk," *BMJ open*, vol. 9, no. 3, p. e025227, 2019.
[8] P. Moeskops, J. M. Wolterink, B. H. van der Velden, K. G. Gilhuijs, T. Leiner, M. A. Viergever, and I. Išgum, "Deep learning for multi-task medical image segmentation in multiple modalities," in *International Conference on Medical Image Computing and Computer-Assisted Intervention*. Springer, 2016, pp. 478–486.
[9] Ø. Kjerland, "Segmentation of coronary arteries from ct-scans of the heart using deep learning," Master's thesis, NTNU, 2017.
[10] J. M. Wolterink, T. Leiner, and I. Išgum, "Graph convolutional networks for coronary artery segmentation in cardiac ct angiography," in *International Workshop on Graph Learning in Medical Imaging*. Springer, 2019, pp. 62–69.
[11] B. Kong, X. Wang, J. Bai, Y. Lu, F. Gao, K. Cao, J. Xia, Q. Song, and Y. Yin, "Learning tree-structured representation for 3d coronary artery segmentation," *Computerized Medical Imaging and Graphics*, vol. 80, p. 101688, 2020.
[12] O. Ronneberger, P. Fischer, and T. Brox, "U-net: Convolutional networks for biomedical image segmentation," in *International Conference on Medical image computing and computer-assisted intervention*. Springer, 2015, pp. 234–241.
[13] F. Isensee, P. Kickingereder, W. Wick, M. Bendszus, and K. H. Maier-Hein, "Brain tumor segmentation and radiomics survival prediction: Contribution to the brats 2017 challenge," in *International MICCAI Brainlesion Workshop*. Springer, 2017, pp. 287–297.
[14] T. Nemoto, N. Futakami, M. Yagi, A. Kumabe, A. Takeda, E. Kunieda, and N. Shigematsu, "Efficacy evaluation of 2d, 3d u-net semantic segmentation and atlas-based segmentation of normal lungs excluding the trachea and main bronchi," *Journal of radiation research*, vol. 61, no. 2, pp. 257–264, 2020.
[15] F. Tian, Y. Gao, Z. Fang, and J. Gu, "Automatic coronary artery segmentation algorithm based on deep learning and digital image processing," *Applied Intelligence*, vol. 51, no. 12, pp. 8881–8895, 2021.
[16] W. K. Cheung, R. Bell, A. Nair, L. J. Menezes, R. Patel, S. Wan, K. Chou, J. Chen, R. Torii, R. H. Davies *et al.*, "A computationally efficient approach to segmentation of the aorta and coronary arteries using deep learning," *Ieee Access*, vol. 9, pp. 108 873–108 888, 2021.
[17] X. Xu, T. Wang, Y. Shi, H. Yuan, Q. Jia, M. Huang, and J. Zhuang, "Whole heart and great vessel segmentation in congenital heart disease using deep neural networks and graph matching," in *International Conference on Medical Image Computing and Computer-Assisted Intervention*. Springer, 2019, pp. 477–485.